P2.8

TOTAL SCAN
A FULL VOLUME SCANNING STRATEGY FOR WEATHER RADARS

Dominik Jacques*, I. Zawadzki
J. S. Marshall Radar Observatory, McGill University, Canada

1. INTRODUCTION

The most common way to make measurements with a weather radar is to have its antenna perform complete rotations at a number of predetermined elevations. The 'volume scans' thus produced seldom include elevations higher than 30°.

This decision is made as a compromise between the time required for the completion of volume scans and the atmospheric volume covered. At high elevations, most of the radar beam is above the tropopause and weather echoes. Scanning there takes as much time as other elevations but only a very small portion of the atmosphere is covered. Considering that the most common product of radar measurements consists in 2D maps of precipitation coverage, neglecting high elevation is justified.

Because of advances in the assimilation of radar data, it is now possible to envision a future where the main purpose of radar measurements would be to provide information to assimilation systems for atmospheric state estimations at mesoscale. An example of such a system is discussed elsewhere in this conference (Zawadzki et al. 2009). In this context, 3D fields of wind, water content and pressure could well replace the 2D maps of reflectivity so common now.

If the end product is to change, perhaps the scanning strategy should also be reconsidered. Here we introduce a 'Total' scanning strategy where the complete volume around a radar is scanned including a rotation of the antenna at vertical incidence.

The Total scanning strategy will prove beneficial to assimilation systems. In many respects, producing an atmospheric analysis from radar measurements is similar to a regression process. We know from regression theory that the regressands will suffer from variance inflation if the regressors are correlated. That is, the uncertainty of the estimated variables increases when the predictor variables share explanatory power. We also know from Berenguer and Zawadzki (2008) that the errors of radar measurements are strongly correlated in space. Scanning the whole volume around a radar, where measurements are less likely to share explanatory power can only be beneficial to assimilation systems. Additionally, the very nature of high elevation and vertical measurements is different from horizontal scans. This will also reduce the correlation of the predictor variables.

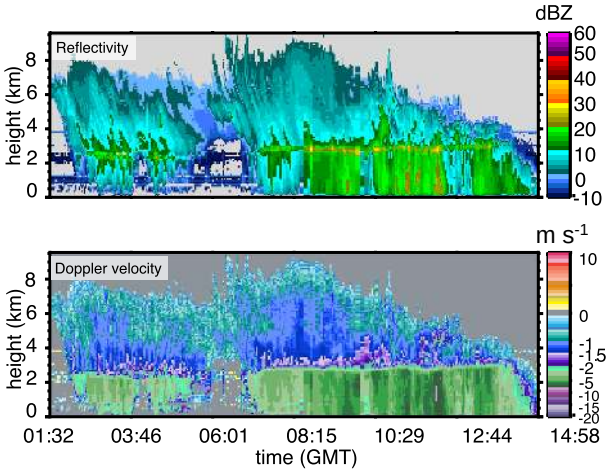

Figure 1: Vertically retrieved Reflectivity (top) and Doppler velocity (bottom) by MA1 on June 4, 2008.

The goal of the present study is to test new applications made possible by adding high-elevation and vertical PPIs to more traditional volume scans.

2. VERTICALLY POINTING MEASUREMENTS

The first Total scan experiments were performed with a X-band radar from the CASA project. The vertical scans were averaged to produce time-height plots of reflectivity and Doppler velocity as depicted in Fig. 1. In this figure, we can see some of the typical features usually observed with vertically pointing radars. Snow trails, originating from moving snow-generating cells are easy to distinguish at altitudes between 4 and 8 km around 8:00 GMT.

*Corresponding author address: Dominik Jacques, Univ. McGill, Dept. Atmospheric and Oceanic Sciences, Montreal, Qc, H3A 2K6; e-mail: dominik.jacques@mail.mcgill.ca.

We can also identify the melting layer, characterized by peak reflectivity values and a sharp increase of Doppler velocity throughout the event.

In the past, vertically pointing radars have mostly been used in research environments for cloud physics and dynamics studies. Vertical incidence measurements contain an intricate blend of information from the size distribution of hydrometeors, their phase and vertical wind motions. For example, Zawadzki et al. (2001) were able to distinguish secondary ice generation from supercooled drizzle by considering vertical incidence Doppler spectra. So far it has been impossible to sort out this information without the use of constraining assumptions or measurements from other sources. Perhaps vertical measurements could be used as additional constrains in assimilation systems.

3. CALIBRATION OF Z_{DR} FROM VERTICAL INCIDENCE MEASUREMENTS

Vertical incidence measurements can also be used for the calibration of Z_{DR}. This technique is usually presented as being easy to implement and not requiring much attention (Gorgucci et al. 1992; Bringi and Chandrasekar 2001; Vivekanandan et al. 2003; Hubbert et al. 2003; Ryzhkov et al. 2005; Hubbert et al. 2008).

It is true that theory behind this method is very simple. At vertical incidence, the cross section of raindrops should be independent from the polarization plane so that the measured Z_{DR} should equal 0. In the melting layer and in snow, particles have heterogeneous shapes. Wind shear could then induce preferential orientation of particles that would in turn cause Z_{DR} to differ from 0. This effect can be eliminated by averaging Z_{DR} over a 360° rotation of the antenna. Z_{DR} measured in this fashion should directly yield the calibration bias.

The Total scanning strategy, including periodic rotations of the antenna at vertical incidence, provides a perfect setup to monitor the radar calibration. However, the experiments that were conducted at S-band and X-band have demonstrated the need to perform this calibration with care.

Hubbert et al. (2008) mentioned the need to filter out ground clutter from the calibration procedure. To do so, they proposed a series of thresholds on SNR, LDR and ρ_{hv}. Ground clutter contamination was found to be a major source of problem in measurements from the McGill S-band radar. Unfortunately, the thresholds proposed by Hubbert et al. (2008) could not be applied on this data.

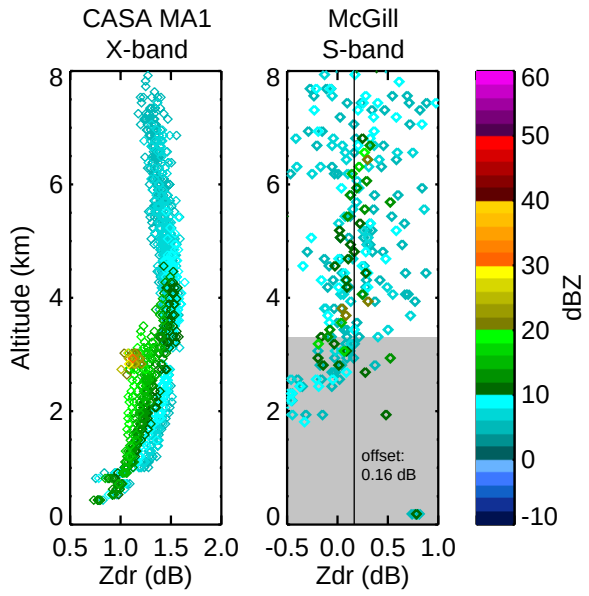

Figure 2: Vertical incidence Z_{DR} as a function of altitude for the McGill S-band and the CASA X-band radars. The color scale indicates the reflectivity at each point, grey shaded area indicate rejected data points due to ground clutter.

Figure 2 shows Z_{DR} as a function of altitude during a one hour period of Total scan for the two radars used in this study. Every data point was averaged over a full rotation of the antenna and the color scale indicates the reflectivity (Z_h) of each point.

For the McGill radar, Z_{DR} was found to be very noisy when reflectivity was lower than 10 dBZ. Ground echoes could also be detected at altitudes lower than 3.3 km. Consequently, the 0.16 dB offset on Z_{DR} was found considering only measurements higher than 3.3 km with reflectivities greater than 10 dBZ.

In the case of the X-band radar, calibration of Z_{DR} was not possible as it showed a strong dependence on the received power. In Fig. 2, this effect can be observed as consistent variations of Z_{DR} as function of reflectivity and altitude. We can speculate that the non-linear response of amplifiers could be causing this dependence.

The much smaller near field at X-band (≈200 m compared with 2000 m as S-band) allows Z_{DR} measurements in most part of the rain below the melting layer. This gives a net advantage to X-band radars for vertical measurements.

Figure 2 illustrates that vertical incidence measurements of Z_{DR} should not only be used for calibration but also to diagnose suspicious behavior of the

radars.

4. WIND PROFILING

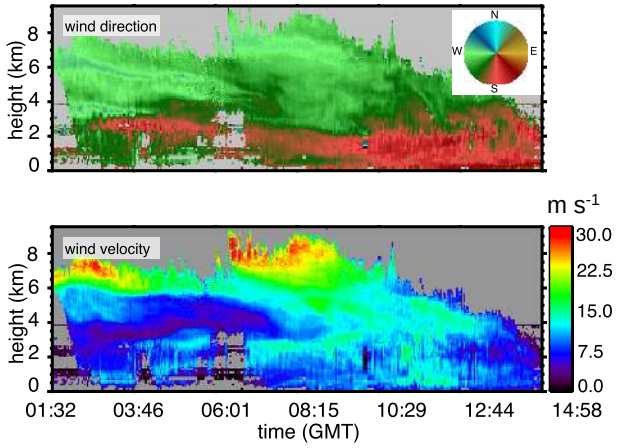

Figure 3: Horizontal wind direction (top) and velocity (bottom) retrieved from 80° VADs on June 4, 2008.

Other than vertical scans, the Total scanning strategy also includes high elevation PPIs. Figure 3 was made from 80° PPIs using VAD.

High elevation PPIs are particularly interesting since the VAD radii are small. The retrieved wind and divergence are then representative of the mesosale conditions in a narrow cone above the radar.

This figure demonstrates the complex multi-layer structure of the atmosphere even for stratiform conditions. At least five layers having a distinct wind direction and velocities can be distinguished between 2:00 and 6:00 GMT. The magnitude of the wind shear observed (sometimes 45° and a few tens of meters per seconds) makes the interpretation of such time-height plots difficult. For this case, one certainly cannot consider time-height plots as being equivalent to measurements through a system moving with constant velocity and direction. An interpretation that could be suggested by the smooth features of vertical incidence reflectivity and Doppler velocity (Fig. 1).

Interesting oscillations in the wind direction coinciding with the melting layer can be clearly observed at 3 km around 2:30 GMT. Perhaps these oscillations are the horizontal manifestations of melting-induced convections as suggested by Atlas et al. (1969). We can also speculate that these oscillations originate from gravity waves modulating the horizontal flow.

These observations could not have been made by looking a vertically retrieved Reflectivity and Doppler velocity of VADs performed at elevations below 30°. Profiles from low elevation VADs (not shown here) show qualitative resemblance with those of Fig. 3 but only the largest features can be seen.

Profiles of horizontal divergence were also retrieved from 80° PPIs (not shown here) but they are very noisy. Perhaps the structure of divergence at this scale is so small that the 3-min resolution is not sufficient to capture it. It is also possible that errors such as inhomogeneous terminal velocity or instrumental noise overwhelm the divergence signal. At this moment, it is unclear which of these two effects dominates.

5. DIFFERENTIAL REFLECTIVITY AND VERTICAL DOPPLER VELOCITY

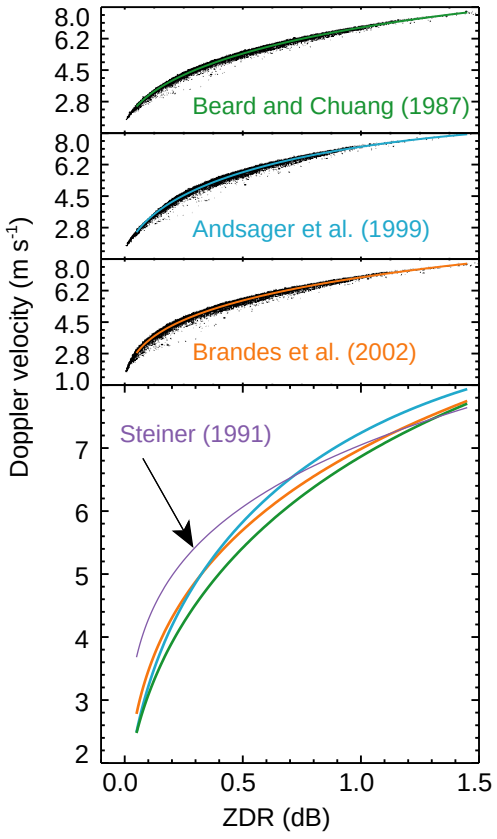

Figure 4: Effect of the drop deformation model on the V_{Dop}-Z_{DR} relation. Scatter plots and the best fit for three deformation relation are presented in the top plots. The same curves are replotted against the relation found by Steiner (1991) in the bottom plot.

Steiner (1991) demonstrated the strong relation between reflectivity weighted Doppler velocity at vertical incidence (V_{Dop} hereafter) and Z_{DR}. He also proposed to use this relation to estimate vertical velocities w in the atmosphere. Two radars were needed for the setup he suggested. A first one, vertically pointing, measuring V_{Dop} and a second, some distance away, measuring Z_{DR} by performing RHIs above the first radar. The difference between V_{Dop} measured at vertical incidence and the one expected from measurement of Z_{DR} would then lead to estimations of w.

The Total scanning strategy allows vertical velocity estimates using a single scanning radar. V_{Dop} could be measured during the vertical scanning periods and Z_{DR} estimated by performing averages over complete antenna rotations at different elevations. Under the assumption that DSDs and vertical motions are horizontally homogeneous, w could be estimated. For stratiform conditions and relatively small VAD radii, the horizontal homogeneity assumption should apply.

Vertical wind retrievals are not attempted here. However, in preparation for such experiment we reproduced Steiner's analysis to test the sensitivity of the V_{Dop}-Z_{DR} relation to the choice of different deformation relations. Evaluating this error is important since it will limit the accuracy of vertical wind estimates.

Figure 4 was produced using a data set of 15 000 one-minute disdrometer measurements, the scattering model by Mishchenko et al. (2000) and the deformations relations by Beard and Chuang (1987), Andsager et al. (1999) and Brandes et al. (2002). These three deformation relations include the effect of drop oscillations which reduce Z_{DR} values for small drops (Goddard and Cherry 1984). In a recent study using a video disdrometer, Thurai and Bringi (2005) demonstrated that these three relations were mostly accurate with the one by Brandes et al. (2002) best matching the measurements.

We used the difference between these models as a proxy for possible model errors or natural variability of the raindrop deformations. It was found that changing the deformation relation introduced an uncertainty in the order of 0.5 m s^{-1} in V_{Dop}. An error approximately equal to the one introduced by the natural scatter around this relation. Given this uncertainty, it may be difficult to estimate vertical velocities in stratiform systems where w is expected to be smaller than 0.5 m s^{-1}.

Steiner's original relation was also plotted in Fig. 4. The discrepancy between this relation and the ones we derived is particularly apparent for Z_{DR}<0.7 dB. We attribute this to the different drop deformation, disdrometer, and data set utilized.

It was found that the scatter around the V_{Dop}-Z_{DR} relation was mainly due to event-to-event variability of DSDs. For individual events, the scatter was smaller than 0.1 m s^{-1}. This opens interesting perspectives for the accurate estimation of vertical wind motions when disdrometric data is also available. This could also allow the estimation of V_{Dop} in the complete volume around the radar, information that could also be used as an additional constraint to assimilation systems.

6. SUMMARY

In this study, we introduced a scanning strategy where measurements are made in the full volume around a weather radar including a complete rotation of the antenna at vertical incidence. We have shown examples of time-height plots made by concatenating many of these vertical measurements.

Unexpectedly, we discovered that vertically retrieved Doppler velocity could be used to diagnose misreadings of the antenna elevation. We came to this conclusion while investigating the systematic presence of a VAD signature in vertical measurements. The simplest explanation to these VADs was the presence of an offset between the radar antenna elevation and the zenith. We could then estimate the 'real' antenna elevation to be ≈91°. It was later confirmed that a sliding strap was causing this offset (Eric Lyons, personal communication).

Polarimetric measurements at vertical incidence also allow the calibration of Z_{DR}. This application is of particular importance because once Z_{DR} is properly calibrated, reflectivity can also be calibrated using self-consistency methods (Gorgucci et al. 1992; Scarchilli et al. 1996; Illingworth and Blackman 2002; Vivekanandan et al. 2003). One of the difficulty for the calibration of Z_{DR} is the contamination by ground echoes. Identification of contaminated data points was shown to be a very important aspect of this procedure.

We also demonstrated the usefulness of using high-elevation PPIs to produce horizontal wind profiles from VAD. Performing these retrievals at high elevation reveals fine scale structures that cannot be observed by other means.

We then explored the possibility of estimating vertical wind motions through the use of the V_{Dop}-Z_{DR} relation introduced by Steiner (1991). We found this relation to be very sensitive to the drop deformation relation used in its derivation. This factor and the natural scatter around the relation will make vertical

velocity estimations in stratiform cases difficult at best. However, the scatter of the V_{Dop}-Z_{DR} relation becomes very small if individual rain events are considered. This opens new possibilities for V_{Dop} estimations in the volume around a radar.
Additional experiment with the total scanning strategy are scheduled with the McGill S-band radar.

Acknowledgement

Special thanks to Eric Lyons for providing the data from the MA1 radar. Thanks also to Valliappa Lakshmanan of NSSL for making his AMS Latex style file available on the web.

References

Andsager, K., K. V. Beard, and N. F. Laird, 1999: Laboratory measurements of axis ratios for large raindrops. *Journal of the Atmospheric Sciences*, **56**, 2673–2683.

Atlas, D., R. Tatehira, M. W. Srivastava, R. C., and R. E. Carbone, 1969: Precipitation induced mesoscale wind perturbations in the melting layer. *Quarterly Journal of the Royal Meteorological Society*, **95**, 544–560.

Beard, K. V. and C. Chuang, 1987: A new model for the equilibrium shape of raindrops. *Journal of the Atmospheric Sciences*, **44**, 1509–1524.

Berenguer, M. and I. Zawadzki, 2008: A study of the error covariance matrix of radar rainfall estimates in stratiform rain. *Weather and Forecasting*, **23**, 1085–1101.

Brandes, E. A., G. Zhang, and J. Vivekanandan, 2002: Experiments in rainfall estimation with a polarimetric radar in a subtropical environment. *Journal of Applied Meteorology*, **41**, 674–685.

Bringi, V. N. and V. Chandrasekar, 2001: *Polarimetric Doppler radar, principles and applications*. Cambridge University Press.

Goddard, J. W. F. and S. M. Cherry, 1984: The ability of dual-polarization radar (copolar linear) to predict rainfall rate and microwave attenuation. *Radio Science*, **19**, 201–208.

Gorgucci, E., G. Scarchilli, and V. Chandrasekar, 1992: Calibration of radars using polarimetric techniques. *IEEE transactions on geoscience and remote sensing*, **30**, 853–858.

Hubbert, J., F. Pratte, M. Dixon, and R. Rilling, 2008: The uncertainty of z_{DR} calibration. *Preprints of the 33rd radar conference*.

Hubbert, J. C., V. N. Bringi, and D. Brunkow, 2003: Studies of the polarimetric covariance matrix. part i: Calibration methodology. *Journal of Atmospheric and Oceanic Technology*, **20**, 696–706.

Illingworth, A. J. and T. M. Blackman, 2002: The need to represent raindrop size spectra as normalized gamma distributions for the interpretation of polarization radar observations. *Journal of Applied Meteorology*, **41**, 286–297.

Mishchenko, M. I., J. W. Hovenier, and L. D. Travis, 2000: *Light Scattering by Nonspherical Particles*. Academic Press, New York, 690pp.

Ryzhkov, A. V., S. E. Giangrande, V. M. Melnikov, and T. J. Schuur, 2005: Calibration issues of dual-polarization radar measurements. *Journal of Atmospheric and Oceanic Technology*, **22**, 1138–1155.

Scarchilli, G., V. Gorgucci, V. Chandrasekar, and A. Dobaie, 1996: Self-consistency of polarization diversity measurement of rainfall. *Geoscience and Remote Sensing, IEEE Transactions on*, **34**, 22–26.

Steiner, M., 1991: A new relationship between mean doppler velocity and differential reflectivity. *Journal of Atmospheric and Oceanic Technology*, **8**, 430–443.

Thurai, M. and V. N. Bringi, 2005: Drop axis ratios from a 2d video disdrometer. *Journal of Atmospheric and Oceanic Technology*, **22**, 966–978.

Vivekanandan, J., G. Zhang, S. M. Ellis, and D. Rajopadhyaya, 2003: Radar reflectivity calibration using differential propagation phase measurement. *Radio Science*, **38**, 1–14.

Zawadzki, I., K.-S. Chung, A. Kilambi, L. Fillion, and F. F., 2009: From radio detection and ranging (radar) to meso-analysis system (mas). *34th Conference on Radar Meteorology*.

Zawadzki, I., W. Szyrmer, and S. Laroche, 2001: Diagnostic of supercooled clouds from single-doppler observations in regions of radar-detectable snow. *Journal of Applied Meteorology*, **39**, 1041–1058.